Arabian Journal for Science and Engineering
https://doi.org/10.1007/s13369-023-08618-7

RESEARCH ARTICLE-BIOLOGICAL SCIENCES

Reduced Graphene Oxide Modified Enzyme Inhibition-Based Biosensor System for Detection of Paraoxon as a Nerve Agent Simulant

Nimet Yildirim-Tirgil[1,2] · **Meryem Tugce Ozel**[2]

Received: 17 July 2023 / Accepted: 14 December 2023
© The Author(s) 2024

Abstract
Nerve agents, including organophosphorus compounds such as paraoxon, are potent and highly toxic chemicals with grave implications for human health and the environment. In this paper, we present the development of a novel enzyme inhibition-based biosensor for the sensitive and selective detection of paraoxon, which is commonly used as a surrogate for nerve agents. The biosensor employs reduced graphene oxide as a screen-printed electrode surface modification nanomaterial, leading to increased surface electroactivity and, thus, more sensitive detection. The biosensor exhibits a low detection limit of 0.56 pg/ml (limit of detection, LOD) and 1.25 pg/ml (limit of quantification, LOQ), highlighting its high sensitivity for trace-level analysis of nerve agents in complex sample matrices. Our biosensor demonstrates remarkable selectivity for paraoxon, with minimal interference from other non-target chemicals. Stability and repeatability tests reveal that the system maintains its performance integrity over a 45-day period and consistently produces readings with a margin of error of only 5%. Real sample testing in river water, wastewater, and tap water further confirms the biosensor's practical utility, with recovery percentages ranging from 84 to 115%. This biosensor represents a significant advancement in biosensor technology, facilitating the rapid, cost-effective, and reliable detection of toxic substances in real-world scenarios.

Keywords Biosensor · Paraoxon · Nerve agent · Electrochemistry · Graphene oxide · Bioanalytical techniques

1 Introduction

Nerve agents represent a highly potent class of chemical agents renowned for their effectiveness. They derive their name from their pronounced neurotoxic effects, primarily within the nervous tissue. These neurotoxic nerve agents typically belong to the organophosphorus compound family, characterized by their persistence and ease of dispersion. Despite their toxicity, their primary mode of action involves serving as predominantly irreversible acetylcholinesterase inhibitors. Chemical substances that exhibit foundational traits, such as lethality to humans and other organisms, inflicting severe harm and incapacitating them by disrupting their biological functions, possess significant toxicity potential. These substances are resilient against environmental factors and offer cost-effective production, rendering them commonly categorized as chemical weapons. [1].

Organophosphate nerve agents, including Soman (GD), sarin (GB), VX, and tabun (GA), induce covalent modifications of enzymes, particularly at the active site's serine residue responsible for catalytic activity [2]. Cholinesterase group enzymes, particularly acetylcholinesterase (AChE), serve as the primary targets of organophosphate agents. The acute toxic effects of these agents result from the irreversible modification of AChE in nerve tissue, causing a loss of its catalytic function. This modification impedes the degradation of acetylcholine within the tissue, leading to ongoing interactions with its receptors [3]. Thus, AChE enzyme inhibition by these OP pesticides and nerve agents was frequently employed to construct an enzymatic biosensor device for detecting these harmful compounds. The signal produced by AChE inhibition-based nerve agent biosensors is inversely proportional to the concentration of the OP chemical, or, to put it another way, more poisonous compound concentration results in weaker signals [4].

✉ Nimet Yildirim-Tirgil
nyildirimtirgil@ybu.edu.tr

1 Biomedical Engineering Department, Faculty of Engineering and Natural Sciences, Ankara Yildirim Beyazıt University, Ayvalı Mh. Takdir Cad.150 Sk. No:5 Etlik-Kecioren, 06010 Ankara, Turkey

2 Metallurgical and Materials Engineering Department, Faculty of Engineering and Natural Sciences, Ankara Yıldırım Beyazıt University, Ankara, Turkey

Published online: 19 January 2024

Because of the high toxicity of OP pesticides and nerve agents, there is an emergency need for detection tools that are fast, sensitive, reliable, and cost-effective for environmental, safety, and biomedical monitoring [5]. In order to perform various analytical techniques, high-performance liquid chromatography, gas chromatography, mass spectrometry, enzyme-linked immunosorbent assay, capillary electrophoresis, and surface-enhanced Raman scattering spectroscopy have all been developed recently [5]. These methods are sensitive and selective, but they have limitations that prevent them from being used for on-site analysis, especially in urgent situations like accidental pesticide discharges [4]. These limitations include expense, the requirement for skilled staff, and the lengthy pretreatment process. As a result, simple, sensitive, portable, and low-cost methods for detecting OP residues in situ are in high demand [6].

To address the challenges mentioned above, promoting biosensor development has become imperative. Biosensors, characterized by their simplicity, sensitivity, low developmental cost, and user-friendly nature, present a viable solution. These devices are designed to be easily handled by individuals without specialized expertise, making them accessible to a wide range of users. A typical biosensor consists of three key components: a biological recognition element, a transducer, and a signal detector. The biological recognition element plays a pivotal role, requiring exceptional specificity to accurately detect the analyte in diverse samples [7–9]. This emphasis on specificity ensures the biosensor's efficacy in various applications, contributing to their growing prominence as versatile tools in analytical and environmental fields.

Enzyme-based biosensors, due to their unique characteristics, such as increased sensitivity, repeatability, and high specificity, offer immense promise for bioanalysis [8–10]. Enzyme-based biosensors measure the response of enzyme-catalyzed reactions; each physical measurement is related to the rate of this reaction and is used in the determination. Upon various physical detection mechanisms, electrochemical systems allow for the quantitative or semi-quantitative assessment of target analytes. Comprising biorecognition elements, signal transduction components, and data analysis tools, these biosensors are cost-effective, remarkably sensitive, and amenable to miniaturization [11, 12]. Traditional electrodes come with the drawback of necessitating relatively large sample volumes and complex cell configurations, making them unsuitable for "in-field" applications. In response to this challenge, screen-printed electrodes (SPEs) have emerged as excellent alternatives, effectively addressing the limitations associated with conventional electrodes [13].

Nanotechnology represents a highly promising interdisciplinary field encompassing engineering, physics, chemistry, computer science, and medicine [14]. Engineered at the nanoscale, this technology holds promise for augmenting human capabilities through intricate nano-design, exhibiting considerable potential for practical revival. Employing bioanalytical and life technical techniques with precisely controlled dimensions enhances the viability of nanomaterials within living organisms, resulting in diminished losses, heightened selectivity, and improved efficiency compared to conventional nanomaterials [15, 16]. Graphene, a prominent carbon-based nanomaterial extensively utilized in the realms of sensing and biosensing, is particularly recognized for its exceptional electrical conductivity. Graphene derivatives such as graphene oxide (GO) and reduced graphene oxide (rGO) are more commonly employed as the foundation for electrochemical biosensors due to their high electrical conductivity, large surface area, better electrocatalytic activity, and excellent electron transfer rates. It is a promising nanomaterial for developing analytical tools for toxic molecule detection [17]. Additionally, enhanced electrical conductivity leads to hydrophobic rGO surfaces, which are crucial for immobilizing enzymes in biosensor systems [18].

Table 1 compares our developed biosensor with existing paraoxon biosensors based on various methods. Upon comparing an innovatively devised biosensor system in this work with extant technologies, its remarkable sensitivity, stability, and proficiency in conducting real sample tests substantiate its candidacy for on-site detection of paraoxon and various other toxic compounds. The capacity to execute dependable, highly sensitive, and stable measurements within authentic environmental contexts represents a noteworthy advancement in biosensor technology. This biosensor stands poised to enhance safety and environmental monitoring by facilitating the identification of hazardous substances across diverse settings. In the context of this biosensor, including rGO is a crucial component for optimizing the sensing platform. The large surface area and excellent electrical conductivity of rGO are crucial in efficiently immobilizing bioreceptors or sensing elements on the electrode surface. This strategic integration of nanomaterials enhances the sensitivity and specificity of the biosensor and facilitates rapid and precise detection. With an impressively low detection limit of 0.56 pg/ml (2.02×10^{-12} M), it surpasses the capabilities of most biosensor methods detailed in Table 1. Furthermore, its broad detection range of 2–100 pg/ml (7.22×10^{-12} M to 6.30×10^{-10} M) ensures versatility in applications, distinguishing it from other biosensors. Additionally, the biosensor demonstrates exceptional readability, undergoing 10 measurements with a precision of 5%. Notably, its stability over a period of 45 days, with an impressive 85% stability rate, exceeds the durability and reliability of many biosensors. Importantly, the biosensor excels in real sample testing, successfully assessing tap water and wastewater with a recovery rate ranging from 84 to 115%, showcasing its practical efficacy in environmental monitoring. In summary, this

Table 1 Comparison of different biosensor techniques to detect organophosphorus nerve agents

Biosensor Method	Detection limit (LOD)	Detection range	Readability	Stability	Real Sample testing	Refs
Quartz Crystal Microbalance (QCM) based sensor	4.57×10^{-8} M	0.1–10 ppm (0.3–36 μM)	5 times with 4.203×10^{-3}%sd	NA	NA	[19]
Optical biosensors	2.39×10^{-10} M	10^{-10} M to 5×10^{-5} M	6 times with 2.36%%sd	NA	In situ, real-time monitoring of real samples	[20]
Calorimetric biosensors	0.001 μg/ml (1.20×10^{-8} M)	0.001–0.012 μg/ml (1.20×10^{-8}–1.09×10^{-7} M)	NA	10 days	Drinking water	[21]
Enzymatic-Optical biosensors	23×10^{-9} M	10 nM to 50 μM Methyl-Parathion	NA	NA	Tap and river water	[22]
Electrochemical biosensors	0.86 ppb (3.1 μM)	0–3 ppm (0–10.8 μM)	Around 7% of sd	40 days	Two times of Spiked tap water	[23]
Electrochemical biosensors	0.24 nM	5–30 nM acarbosulfan	Around 5%	NA	Rice samples	[24]
Amperometric biosensors	0.212 μM	3.60–21.6 μM	NA	25 days	Milk and tap water	[25]
Fluorescence biosensors	0.22 nM	Trypsin concentration of 0–16 nM	Around 5%	NA	NA	[26]
Voltammetric biosensors	0.45 nM	0.46–1.84 nM paraoxon	NA	60 days	Tap and river waters	[27]
This work	0.56 pg/ml (2.02×10^{-12} M)	2–100 pg/ml (7.22×10^{-12} to 6.30×10^{-10} M)	10 times with %5	45 days with %85 stability	Tap water, wastewater testing with %84–115 recover	

biosensor represents a significant advancement in biosensor technology, combining sensitivity, range, readability, stability, and real-world applicability.

The manuscript introduces a groundbreaking approach to address the urgent need for fast, sensitive, and reliable detection of nerve agents, particularly focusing on the organophosphorus compound paraoxon. The established system involves the development of a novel enzyme inhibition-based biosensor utilizing reduced graphene oxide (rGO) as a screen-printed electrode (SPE) surface modification nanomaterial. This modification significantly enhances surface electroactivity, leading to a substantial increase in sensitivity for paraoxon detection. The unique features of the biosensor, such as its exceptional sensitivity, stability, and real sample testing capabilities, position it as a promising tool for detecting paraoxon and other toxic compounds in a variety of real-world scenarios.

2 Materials and Methods

2.1 Chemicals and Reagents

Reduced graphene oxide was purchased from Nanografi Nano Technology Turkey (Distribution Office), Turkey. Chitosan, acetylcholinesterase enzyme (AChE), acetylcholine chloride (ACH) enzyme, choline oxidase enzyme (ChO), KCl, phenol, catechol, gallic acid, and hypoxanthine and Paraxon were purchased from Sigma-Aldrich, Germany. Phosphate buffer (PBS) was prepared using di-potassium hydrogen phosphate and potassium dihydrogen phosphate. 5 mM $[Fe(CN)_6]^{3/4}$, which contained 0.1 M KCl solution, was prepared in the laboratory to ascertain the surface activity and conductivity of the electrode.

2.2 Instruments, Surface Characterization, and Electrochemical Methods

Using an electrochemical workstation called Emstat4s (PalmSens BV, Netherlands), electrochemical techniques

such as electrochemical impedance spectroscopy (EIS), cyclic voltammetry (CV), and differential pulse voltammetry (DPV) tests were performed. The electrochemical measurements were recorded using screen-printed electrodes (SPE from DropSens, Switzerland) that the SPE three-electrode system consisted of a carbon plate as the counter electrode (CE), carbon plate as the working electrode (WE), and Ag/AgCl as the reference electrode (RE).

CV method for electrode surface characterization depends on the electroactive surface areas were performed by scanning the surface with different scan rates between 10 mv/sec and 250 mV/sec in 5 mM $Fe(CN)_6^{3-}/Fe(CN)_6^{4-}$ containing 0.1 M KCl solution. DPV method were performed during the biosensor development and performance optimization steps. EIS measurements were also conducted after each modification of the SPE in KCl solution (0.1 M) containing mM $[Fe(CN)_6]^{¾}$, 10 mV amplitude, and a frequency range of 0.1–100.000 Hz.

The spectral study of blank and modified SPE surfaces were recorded by using Renishaw inVia RM1000 Raman microscope, using 532 nm laser excitation wavelength. Hitachi S-4700 scanning electron microscope was used for observation of surface morphology. The X-ray diffraction (XRD) patterns were recorded by using D/MAX-2500 X-ray diffractometer, with Cu Kα radiation (λ = 1.5406 Å).

2.3 Preparation and Characterization of rGO Modified Electrodes

Surface modifications of carbon SPEs were made by drop casting and electrodeposition methods with 1 mg/ml concentration of rGO that was prepared in distilled water and sonicated (10 min) to make rGO homogeneous in an aqueous solution. The prepared solution was dropped onto the carbon SPE electrode surface during drop-casting and left to dry at room temperature for 2 h. The electrodeposition method was also performed with 1 mg/ml rGO at − 1.5 V for a period of 5 min, as mentioned in the literature before.

Surface characterization and optimization of the rGO modification method experiments were performed after this point.

The Randles–Sevcik equation was employed in cyclic voltammetry experiments with different scan rates to demonstrate the link between peak current (*ip*), scan rate (*v*), and electroactive surface area. With this calculation, the active surface area of the blank SPE and rGO modified surfaces were calculated and compared.

$$\text{Slope} = \left(\frac{i}{\sqrt{v}}\right) = k.n^{3/2}.A.\sqrt{D}.C_{\text{FC}}$$

where $n = 1$ (number of electrons transferred in the redox event). $k = 2.69 \times 10^5$ Cmol^{-1} $\text{V}^{-½}$ (constant). $D = 0.16 \times 10^{-6}$ cm^2 s^{-1} (diffusion coefficient for the redox couple). A = Electroactive electrode Area (cm^2). $C_{\text{FC}} = 0.000005$ mol/cm^3 (redox couple concentration). V = 10 mV/sec to 250 mV/sec (scan rates).

2.4 Enzyme Immobilization

Acetylcholinesterase and colin oxidase enzymes were dissolved in PBS with concentrations of 2 mg/ml of each, and the prepared enzyme mixture was added to 2% of the chitosan solution (in acetic acid) to get a 1:1 ratio of the mixture. The enzymes/chitosan mixture was then dropped onto the rGO-modified electrode surface and dried at room temperature for 2 h. Chitosan ensures the immobilization of enzymes and their adsorption to the surface. EIS measurements and SEM imaging were performed to analyze the prepared surfaces.

2.5 Biosensor Preparation and Assay Procedure

After enzyme immobilization onto the modified electrode surface, 50–800 μM acetylcholine chloride (Ach) was injected into the surface. The immobilized enzyme started to catalyze ACh to form hydrogen peroxide in two steps, as seen in Fig. 1. The final product, hydrogen peroxide, could be detected electrochemically within a suitable potential. DPV measurements were performed, and as a result of the analysis, the peak height was calculated for each ACh concentration. The saturation of the enzyme-immobilized electrode surface determined the optimum level.

After the ACh concentration optimization experiments, different concentrations of paraoxon were mixed with the optimum ACh and added to the surface of enzyme-modified electrodes to observe the enzyme inhibition effect. The decrease of the enzyme–substrate pair detected signal was investigated (Fig. 2D). Relative signal differences for each concentration of paraoxon were calculated as follows;

I_0: Peak height with optimum acetylcholine concentrations.

I_1: Peak height with paraoxon addition.

ΔI: $I_0 - I_1$.

$\Delta I/I_0$ (relative signal difference): The data used in the biosensor performance optimization and sample testing.

Different concentrations of paraoxon (2–400 pg/ml) were tested by the developed biosensor system, as shown in Fig. 2, and a calibration curve was observed.

2.6 Optimization of the Performance Conditions

2.6.1 pH Optimization

The activity of an enzyme attached to any immobilization matrix or the electrode surface in biosensors significantly impacts the biosensor's performance. DPV experiments

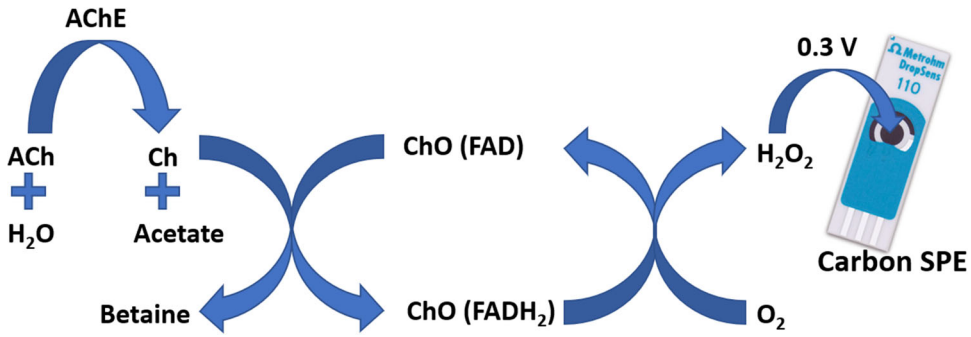


Fig. 1 Reaction scheme for the AChE and ChO enzyme activated electrochemical ACh determination

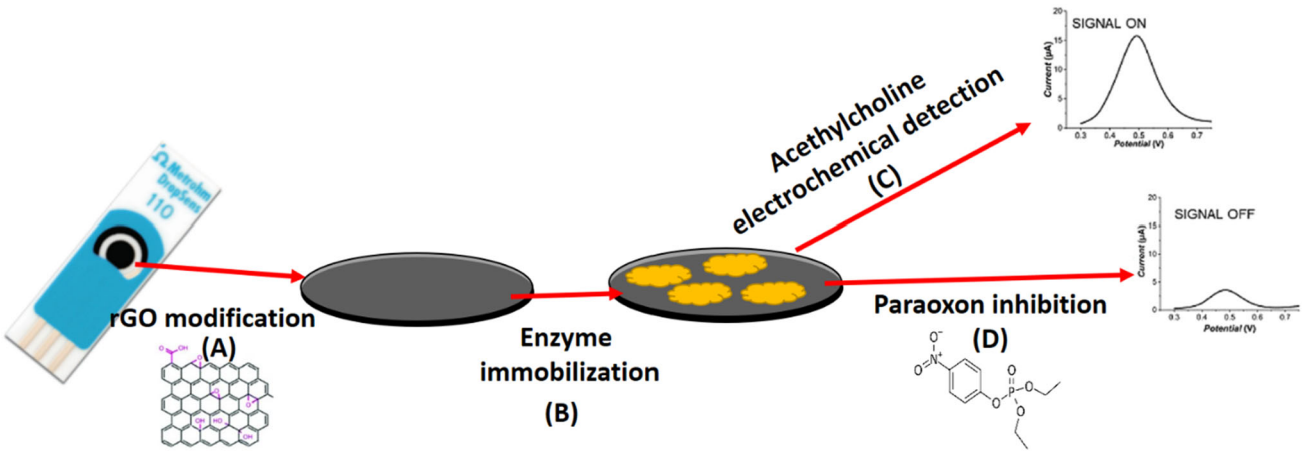


Fig. 2 General working principle of the biosensor method, including enzyme inhibition-based paraoxon analysis. **A** is the surface modification, **B** is enzyme immobilization, **C** is the signal with ACh, and **D** is the signal with paraoxon addition

investigated the dependency of the electrochemical signal on pH at pHs ranging from 6.0 to 8.0 in PBS, having an ideal concentration of ACh (800 M) to ensure the highest analytical response from the constructed biosensor electrode.

2.6.2 Selectivity

Selectivity refers to a bioreceptor's ability to detect a specific analyte in a sample containing other additives and contaminants. To prove the selectivity in the prepared biosensor system, non-target molecules such as phenol, catechol, gallic acid, and hypoxanthine were tested with paraoxon at the 20 pg/ml concentration, and the DPV measurements were compared.

2.6.3 Repeatability and Stability

To prove the reproducibility of these experimental studies, 10 different experiments were carried out under the same conditions with the 20 pg/ml of paraoxon concentration. The results were evaluated to detect the standard deviation (sd) of the developed biosensor system.

The ready-to-use electrodes (rGO modified and enzyme immobilized) were stored at 4 °C for 45 days and tested with 100 pg/ml of paraoxon concentration weekly. The system's stability was determined by comparing the weekly results with those obtained on the first day.

2.7 Real Sample Testing

To further demonstrate the applicability of the developed biosensor, the recovery test was studied by adding paraoxon to river water, wastewater, and tap water samples. 5 pg/ml, 20 pg/ml, and 80 pg/ml of paraoxon were added to these water samples and injected onto the electrode surface for electrochemical detection. Recovery and sd % of all three independent experiments for each concentration were calculated.

3 Results and Discussion

3.1 Surface Modification and Characterization

A cyclic voltammogram was used to conduct electrochemical tests on the drop cast and electrodeposited rGO-modified carbon SPE surfaces at potentials ranging from 0.2 to 0.6 V and at various scan rates between 10 and 250 mV/sec. Figure 3

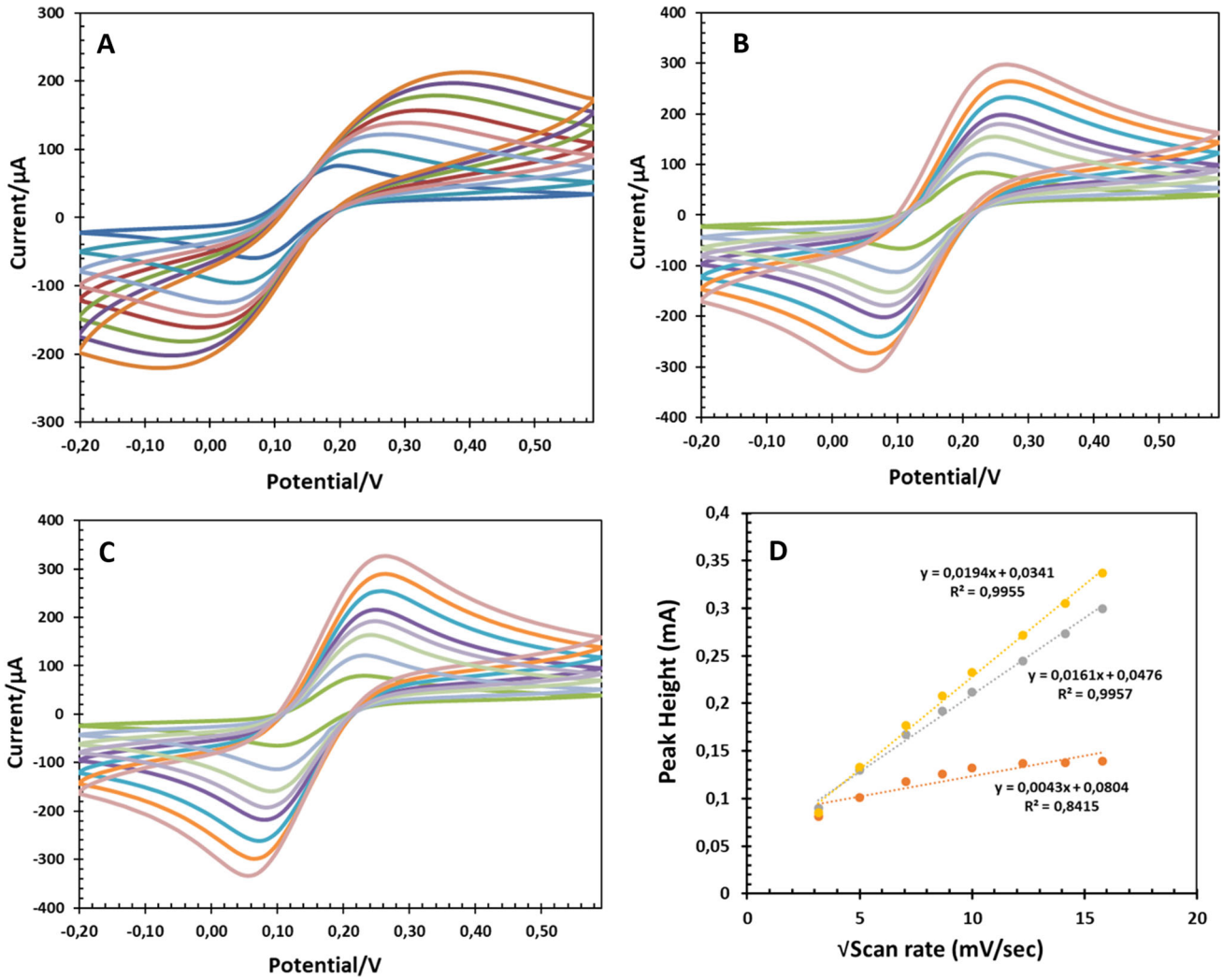


Fig. 3 CV graphs with different scan rates; **A** blank carbon SPE, **B** 1 mg/ml rGO modified surface with electrodeposition, **C** 1 mg/ml rGO modified surface with dop casting method, **D** scan rates versus peak heigh graphs for each tested electrodes

shows the cyclic voltammograms for the bare carbon SPE (A), electrodeposited rGO modified (B), drop casted rGO modified (C) SPE surfaces in 5 mM $Fe(CN)_6^{3-}/Fe(CN)_6^{4-}$ electrolyte solution containing 0.1 M KCl. Figure 3 shows that at a fixed voltage (between 0.2 and 0.6 V), the oxidation and reduction peaks linearly rise with an increase in scan rate. It was seen that the current value for both oxidation and reduction increased as the scan rate increased. A graph between the oxidation current and the square root value for the scan rate was constructed to analyze the steady electron-transfer kinetics for a quasi-reversible process (Fig. 3D). The plotted graph demonstrated that the oxidation current increased as the square root function gradually increased (Fig. 3D). The linear graphs between oxidation peak height and square root value for the scan rates showed good linearity with rGO modification compared to the bare carbon SPE.

Depending on the calculated surface areas with Redness Sevciq Equation by using linear graphs between oxidation peak height and square root value for the scan rates, the bare carbon SPE has 0.3136 cm^2, rGO modification with electrodeposition method has 1256 cm^2, and rGO modification with drop casting method has 1.425 cm^2 respectively.

At a fixed scan rate (100 mV/sec), the oxidation peak current for the bare electrode was observed at 0.09 mA by CV measurements. In contrast, the rGO-modified electrodes with the electrodeposition method increased to 0.025 mA, and drop-casted electrodes with rGO had 0.07 mA of oxidation peak current. The peak height value of the electrode modified with the drop-casting method was higher when compared to the electrodeposition method and the blank electrode. Thus, it can be interpreted that the drop-casting method was most suitable depending on the surface electroactivity.

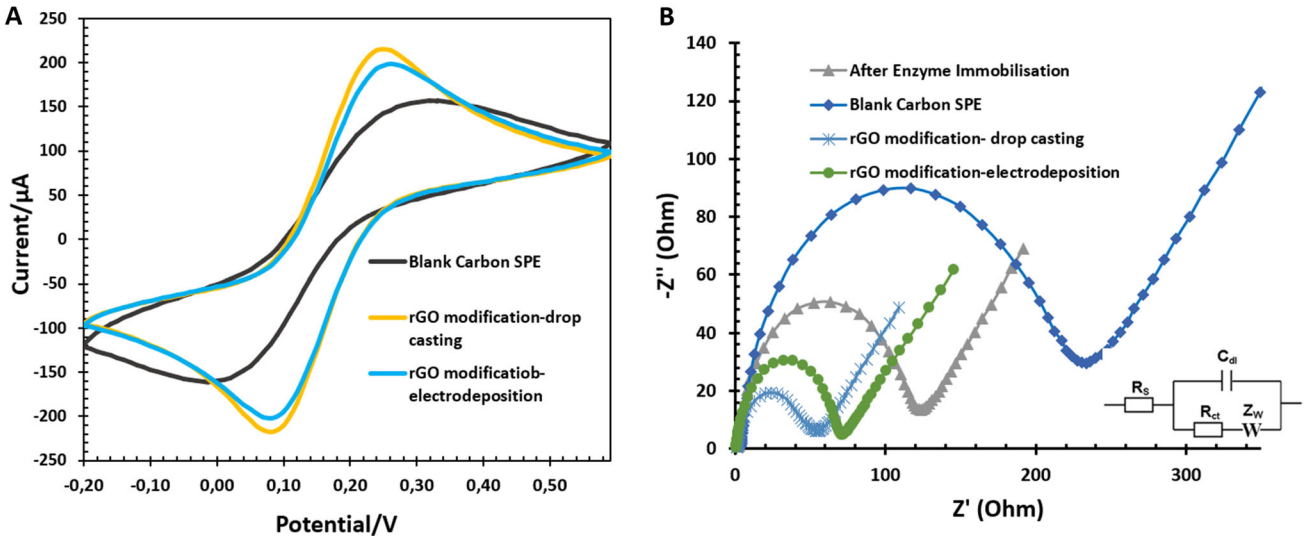


Fig. 4 **A** CV measurements for each modified and blank electrode with 100 mV/sec scan rate in 5 mM FeCN solution in 0.1 M KCl. **B** Electrochemical impedance spectra after each modification in 5.0 Mm [Fe(CN)6] ¾ in KCl solution (0.1 M) containing open circuit mode, 10 mV amplitude, and frequency range of 0.1–100.000 Hz

Using the $Fe(CN)_6$ $^{3/4}$ redox couple as an electrochemical probe, the Nyquist plots of each electrode surface modification were produced in the frequency range of 0.1–100,000 Hz (Fig. 4). The Randles equivalent circuit model, which is depicted in the inset of Fig. 4, B, fits the Nyquist plots (Fig. 4B). The Rct (charge transfer resistance) values for each nanomaterial modification are significantly lower in Fig. 4B, demonstrating that the nanomaterials were successfully accumulated and surface conductance was raised. Considering an inverse ratio between resistance and conductivity, it was concluded that the conductivity of electrode surfaces with a high Rct value is lower.

These results also support the conclusion that rGO modification with the drop-casting method should be the optimum one and depends on the larger surface area, which will have an advantage on electroactivity and a more significant amount of enzyme immobilization on the further step.

Additionally, according to SEM images, changes in the surface morphology and homogeneity of the samples with rGO modification were observed. Figure 5 shows a more porous structure on the surface of the unmodified (blank) carbon SPE electrode sample compared to the surfaces of the rGO-modified samples using the drop-casting method. The surface of the carbon SPE was filled with rGO with good homogeneity, as seen in Fig. 5.

As shown in Fig. 5, D X-ray diffraction (XRD) was applied to acquire detailed information about the microstructure of carbon SPE surface step-by-step modification with rGO and enzyme. One sharp peak can be observed for graphite at $2\theta = 26.62°$ [28]. This peak confirmed the presence of a well-arranged layer structure. After oxygen-containing functional groups were eliminated significantly during the rGO modification, a broader peak can be seen for addition onto the graphite-structured carbon SPE surface at $2\theta = 24.10°$ [28, 29]. A broad peak for rGO implied that the crystal phase was arranged randomly compared to the high crystallization structure of graphite, where a sharp and intense peak can be observed (Fig. 5D). A significant peak intensity change was exhibited in the same position after the enzyme immobilization. The interaction between rGO-modified carbon SPE surface and enzyme protein might cause changes in peak intensity, which changes the graphene structure.

Raman spectroscopy generally characterizes crystal structure, disorder, and defects in graphene-based materials. The Raman spectra of graphite structured carbon SPE surface and rGO modification and enzyme immobilization are shown in Fig. 5E. On the blank carbon SPE surface, we can observe relatively high G band intensity, which represents the pure and dense graphite structure. When the graphite surface was covered with rGO by modification, we can still observe the D and G band, but with a smaller D/G ratio since there is no content of amorphous carbon in the rGO; the D peaks are attributed to the defects [29]. After the enzyme immobilization onto the rGO-modified carbon SPE surface, we can observe the decrease in the G band intensity and maintain the D band because of the surface coverage with the protein-structured enzyme molecule, which has an intense amount of carbon and oxygen atoms [30].

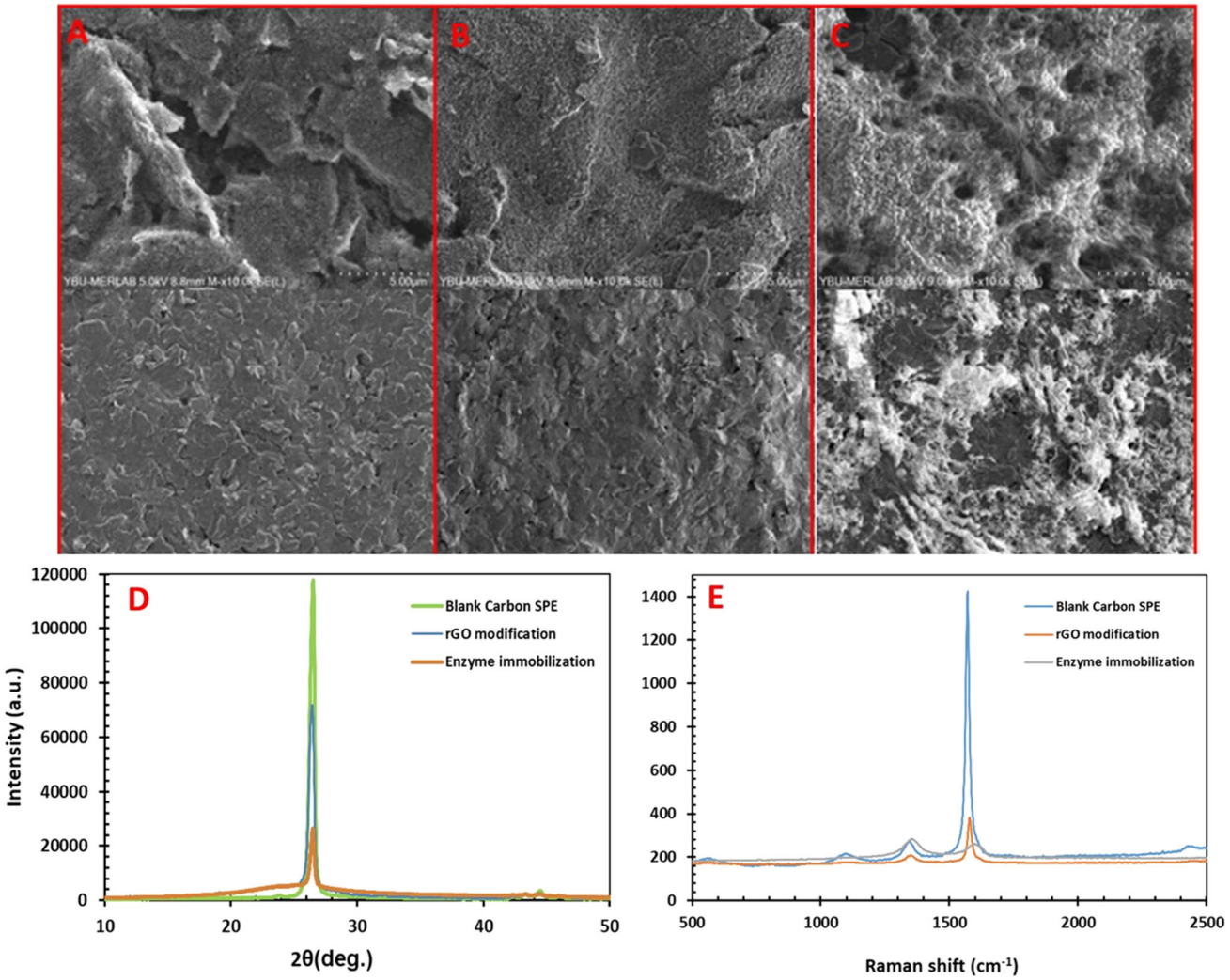


Fig. 5 **A** SEM image of blank carbon SPE surface, **B** SEM image of carbon SPE surface coated with rGO with drop casting method, **C** SEM image when enzyme immobilization is performed on carbon SPE surface coated with rGO, **D** XRD and **B** Raman spectra of carbon SPE surface, after modification with rGO and enzyme immobilization steps

3.2 Enzyme Immobilization

By the EIS measurements, while the Rct value was the highest in the blank SPE, the Rct value of the rGO-modified surface was the lowest (Fig. 4B). When the enzyme is immobilized, the Rct value rises again because a non-electroactive material is added to the surface.

Additionally, as seen in Fig. 5C, enzymes were strongly attached to the rGO-coated SPE electrode surface by the deposition of globular structures of the immobilized enzyme on the rGO-modified electrode, respectively.

3.3 pH Optimization

The prepared biosensor system with acetylcholinesterase/rGO/carbon SPE electrode shows an excellent affinity for acetylcholine chloride. Acetylcholinesterase bioactivity was greatly affected by pH. Results from pH optimization experiments for the operation of this biosensor system containing 800 μM acetylcholine are like the graphic below (as seen in Fig. 6A). The DPV plots demonstrate that the peak current increases from pH 6.0 to 7.5, peaks at pH 7.5, and then decreases at pH 8.0. According to reports, the ideal pH range for AChE is between 7.0 and 8.0 [18]; specific biosensors based on rGO also claim that pH 7.0 is the perfect range for buffer solutions [19, 20]. So, for use in the following tests, pH 7.5 was selected.

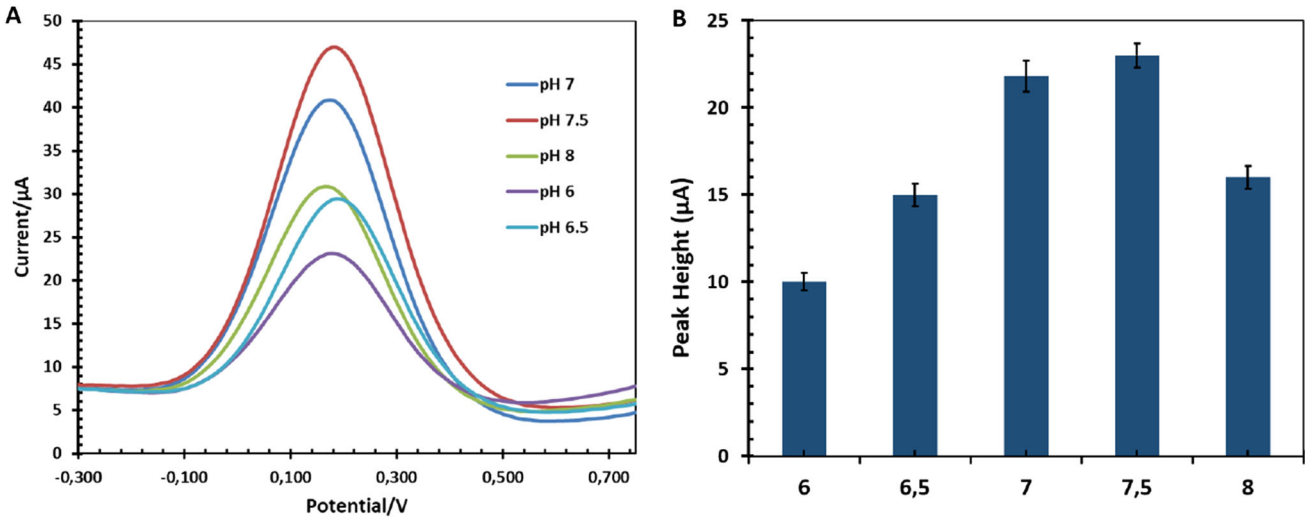


Fig. 6 **A** DPV measurements at different pH ranges of rGO-modified carbon SPE electrode containing 800 µM acetylcholine. **B** Peak height indicating pH determination for optimum operating conditions

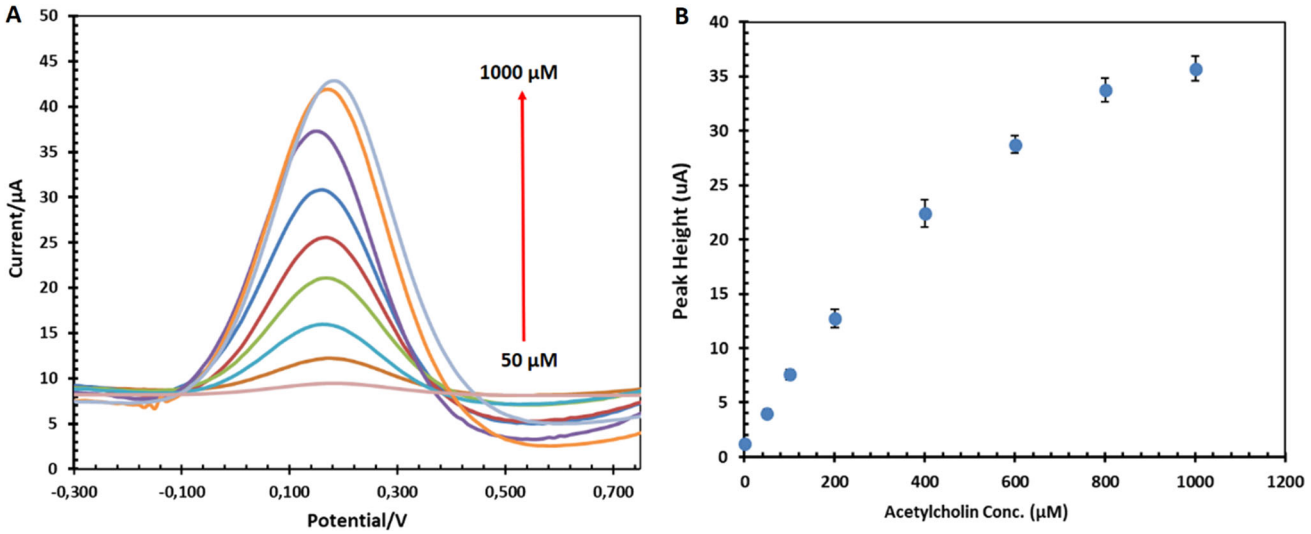


Fig. 7 **A** DPV measurements were made by adding different concentrations of ACh to the prepared electrodes to determine the optimum acetylcholine chloride. **B** Linear curve showing the optimum Acetylcholine concentration of 800 µM

3.4 Acetylcholine chloride (ACh) Saturation Concentration Optimization

Different concentrations of acetylcholine chloride were injected into the rGO-modified and enzyme-immobilized electrode surfaces for optimum saturated acetylcholine chloride determination. Figure 7 shows that with 800 µM ACh, the DPV peak height reached a plateau, and the signal was not increased with further increased concentration. For this reason, paraoxon experiments were continued with the saturated 800 µM of ACh concentrations for further investigations.

3.5 Paraoxon Detection

DPV studies were carried out by adding different concentrations of paraoxon to rGO-modified and enzyme-immobilized carbon SPE electrodes with 800 µM of optimum ACh (as seen in Fig. 8). Considering the DPV results in the tests with different concentrations of paraoxon, it was determined that the amount of peak height observed by ACh was decreased with the increase of paraoxon concentration because of the inhibition of enzyme activity. Figure 8, A is formed by adding different paraoxon concentrations over the optimum acetylcholine concentration (800 µM), and a calibration curve of Paraxon is drawn according to Fig. 8, B under optimum conditions. According to

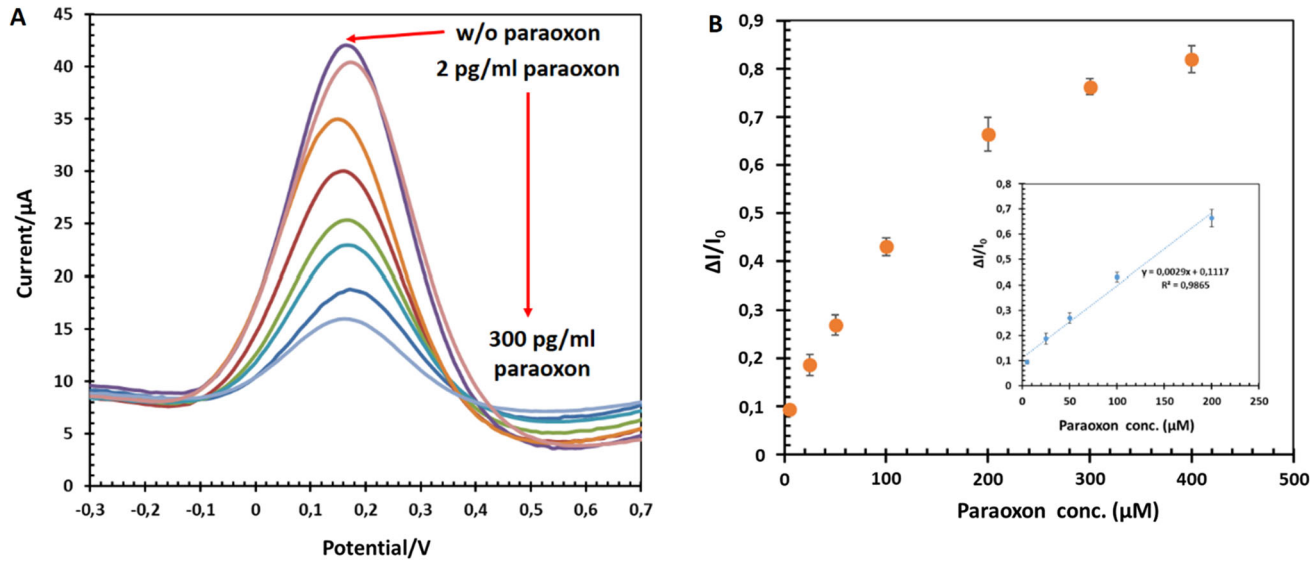


Fig. 8 **A** DPV results by adding different paraoxon concentrations above the optimum acetylcholine concentration (800 µM). **B** Paraxon linear calibration curve under optimum conditions, inner figure; linear range for paraoxon concentration from 2 to 200 pg/ml

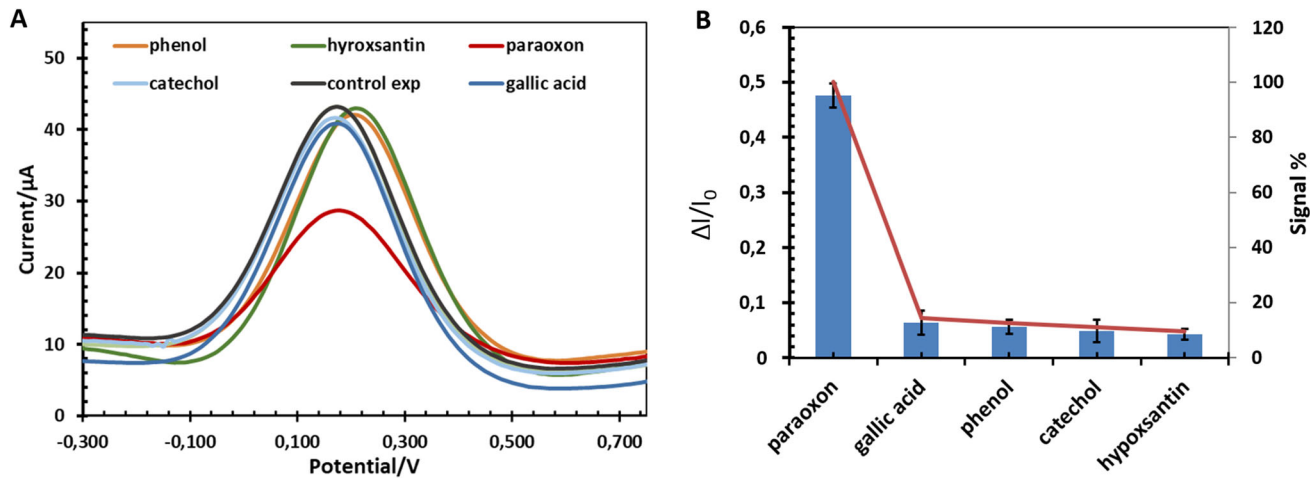


Fig. 9 **A** DPV results of the biosensor's selectivity with phenol, hypoxanthine, paraoxon, gallic acid, catechol, and control experiment. **B** Evaluation of Peak height variation with % of signal for selectivity of different terror agents added under optimum conditions

Fig. 8, B internal figure, Paraoxon concentrations from 2 to 200 pg/ml gave linear results depending on the $\Delta I/I_0$ values.

The standard deviation of 10 current–time measurements of the blank solution was used to compute the detection limit (LOD), which was determined to be 0.56 pg/ml [21]. Additionally, the quantification limit (LOQ) of 1.25 pg/ml was established using the 10/slope method by IUPAC guidelines [22, 23].

3.6 Stability, Repeatability, and Selectivity

3.6.1 Selectivity

One of a biosensor's most crucial characteristics is selectivity, which is the capacity of a bioreceptor to identify a specific analyte in a sample that contains other additives and contaminants. During selectivity experiments, gallic acid, phenol, hypoxanthine, and catechol were employed as substitutes for paraoxon. Figure 9, A explains the application of the DPV technique to assess the sensor response to these chemicals. Notably, there was no noticeable decrease in the DPV signal, indicating an absence of inhibition effects from gallic acid, phenol, hypoxanthine, and catechol in this system. Figure 9,

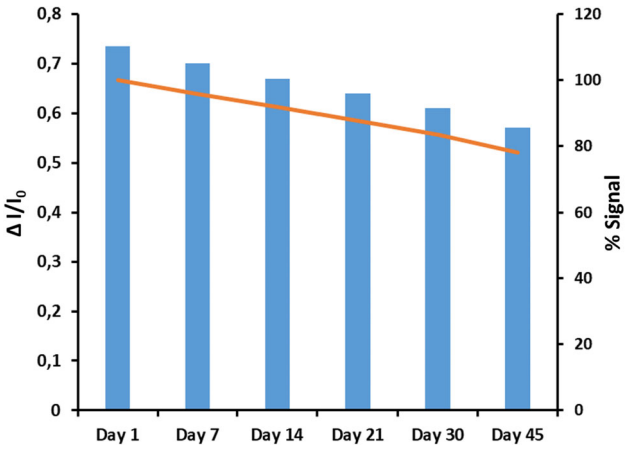


Fig. 10 DPV results were tested under the same conditions but on different days to measure the stability of the same biosensor system. B. Graph showing the varying stability of the biosensor system from day 1 to day 45 under the same conditions

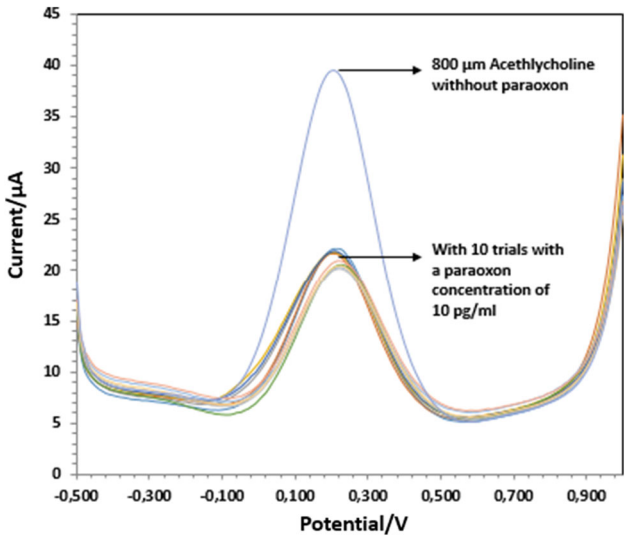


Fig. 11 DPV results showed the biosensor's reproducibility by performing the same biosensor trial on the same day

B provides a comparative analysis, revealing that the electrode containing 800 µM acetylcholine chloride and other chemicals yielded a mere 15% maximum signal response, expressed as ΔI/I0 values, in contrast to the paraoxon signal. This outcome signifies that paraoxon is the specific target for this biosensor system, as the interferent chemicals do not give a significant sensor response. In essence, the biosensor's selectivity is confirmed, highlighting its capability to effectively identify paraoxon within a variety of chemical interferences without notable response deviations.

3.6.2 Stability

The biosensor system prepared with rGO-modified acetylcholine chloride immobilized based on paraoxon detection was stored at 4 °C for 45 days and tested with paraoxon at regular intervals. The stability of the systems was determined by comparing the results obtained depending on the days with the results obtained on the first day. As seen in Fig. 10, the stability of the results obtained with the developed biosensor system was 78% after 45 days.

3.6.3 Repeatability

Repeatability is the ability of a biosensor to deliver the same outcomes for an experimental setup that has been reproduced. The electronics and transducer's accuracy and precision determine repeatability in a biosensor. Accuracy describes the sensor's ability to produce an average value reasonably near the actual value when a sample is measured numerous times. The ability of a sensor to consistently produce similar readings is known as precision. When estimating a biosensor's response, repeatability signals offer high reliability and resilience.

Ten different trials were made on the same day with the produced biosensor, and a standard deviation calculation was created using the DPV technique results. As seen in Fig. 11, the repeatability of the enzyme inhibition-based biosensor system for paraoxon detection resulted in 0.05 sd and 5.45% sd values. Accordingly, the system can perform reproducible analysis with a 5% margin of error.

3.7 Real Sample Analysis

As a result of the experiments, real sample analyses were made in the biosensor system with acetylcholine added on the rGO electrode developed to detect the paraoxon chemical prepared. In the method tested with dirty water and tap water samples, paraoxon was added at 5 pg/ml, 20 pg/ml, and 80 pg/ml, respectively, and tested with the developed system. In the mentioned biosensor performance test step, DVP measurements were made for each added sample, respectively, and ΔI/I0 values were calculated. The amount of paraoxon in each added sample was calculated using the calibration curve drawn earlier. The amounts of paraoxon added and calculated for each sample were compared, and the percentage of recovery values was calculated. All measured samples' accuracy ranged from 84 to 115%, with SD results of 5.6–9.5, respectively, as represented in Table 2.

4 Conclusion

In conclusion, this study presents the development of an enzyme-based biosensor for the sensitive and selective detection of paraoxon, a potent nerve agent. The biosensor utilizes reduced graphene oxide (rGO) surface-immobilized

Table 2 Trial results of improved rGO-based enzyme inhibition-based biosensor system in contaminated water and tap water

	Spiked paraoxon conc.	Calculated paraoxon conc.	% Recovery	% cv
Tap water	5 pg/ml	4,2	84	5.6
	20 pg/ml	21.2	106	7.5
	80 pg/ml	83.3	104	6.8
1. Contaminated water	5 pg/ml	4.3	107	6.8
	20 pg/ml	22.1	110	9.3
	80 pg/ml	84.6	106	8.9
2. Contaminated water	5 pg/ml	4.6	115	7.3
	20 pg/ml	22.3	111	9.3
	80 pg/ml	84.6	106	9.5

acetylcholinesterase enzyme as a recognition element and acetylcholine as a substrate to catalyze the formation of hydrogen peroxide. The system exhibited excellent selectivity for paraoxon, significantly reducing the response to other non-target chemicals and demonstrating its practical utility in detecting specific toxic compounds.

Stability and repeatability are essential characteristics of biosensors, particularly in applications where reliable and consistent results are crucial. The biosensor system displayed outstanding stability over a 45-day period, with a 78% retention of its initial performance. Repeatability tests confirmed the system's ability to produce consistent readings with a margin of error of only 5%. These features make the biosensor reliable and suitable for use in various real-world scenarios. Real sample testing further validated the biosensor's applicability. The system demonstrated its effectiveness in practical environmental monitoring and safety applications by assessing recovery percentages in river water, wastewater, and tap water. Accuracies ranged from 84 to 115%, highlighting its robust performance in complex sample matrices where the biosensor's detection limits of 0.56 pg/ml (limit of detection, LOD) and 1.25 pg/ml (limit of quantification, LOQ) indicate its high sensitivity and suitability for trace-level analysis of nerve agents in various environmental samples.

In summary, this enzyme-based biosensor, leveraging rGO, and acetylcholinesterase enzyme exhibits remarkable potential for on-site detection of nerve agents, such as paraoxon. Its excellent selectivity, stability, repeatability, and sensitivity make it a valuable tool for environmental monitoring, safety applications, and emergency response efforts. Moreover, the study's success in real sample testing, particularly in tap water and wastewater, underscores the practical utility of the biosensor. This knowledge can inform future biosensor fabrication endeavors, emphasizing the importance of designing sensors that excel in controlled laboratory conditions and demonstrate robust performance in real-world environmental matrices. Certainly, the study underscores the significance of incorporating nanomaterials, particularly reducing graphene oxide (rGO), in the design of a novel biosensor system. The use of nanomaterials in biosensor systems generally represents a paradigm shift in sensor technology, harnessing the unique properties of nanoscale materials to enhance sensor performance. The study highlights the pivotal role of nanomaterials, exemplified by reducing graphene oxide, in advancing biosensor technology.

Acknowledgements We want to thank the Ankara Yıldırım Beyazıt University, Department of Scientific Research Project, for supporting this work with the project numbered FYL-2022-2355.

Funding Open access funding provided by the Scientific and Technological Research Council of Türkiye (TÜBİTAK).

Open Access This article is licensed under a Creative Commons Attribution 4.0 International License, which permits use, sharing, adaptation, distribution and reproduction in any medium or format, as long as you give appropriate credit to the original author(s) and the source, provide a link to the Creative Commons licence, and indicate if changes were made. The images or other third party material in this article are included in the article's Creative Commons licence, unless indicated otherwise in a credit line to the material. If material is not included in the article's Creative Commons licence and your intended use is not permitted by statutory regulation or exceeds the permitted use, you will need to obtain permission directly from the copyright holder. To view a copy of this licence, visit http://creativecommons.org/licenses/by/4.0/.

References

1. Mishra, R.K.; Vinu Mohan, A.M.; Soto, F.; Chrostowski, R.; Wang, J.: A microneedle biosensor for minimally-invasive transdermal detection of nerve agents. Analyst **142**(6), 918–924 (2017). https://doi.org/10.1039/c6an02625g
2. Mukherjee, S.; Gupta, R.D.: Organophosphorus nerve agents: types, toxicity, and treatments. J. Toxicol. (2020). https://doi.org/10.1155/2020/3007984
3. Worek, F.; Szinicz, L.; Eyer, P.; Thiermann, H.: Evaluation of oxime efficacy in nerve agent poisoning: development of a kinetic-based

dynamic model. Toxicol. Appl. Pharmacol. (2005). https://doi.org/10.1016/j.taap.2005.04.006
4. Rajangam, B.; Daniel, D.K.; Krastanov, A.I.: Progress in enzyme inhibition based detection of pesticides. Eng. Life Sci. **18**(1), 4–19 (2018)
5. Guo, L., et al.: Colorimetric biosensor for the assay of paraoxon in environmental water samples based on the iodine-starch color reaction. Anal. Chim. Acta **967**, 59–63 (2017). https://doi.org/10.1016/j.aca.2017.02.028
6. Samal, S.; Mohanty, R.P.; Mohanty, P.S.; Giri, M.K.; Pati, S.; Das, B.: Implications of biosensors and nanobiosensors for the eco-friendly detection of public health and agro-based insecticides: a comprehensive review. Heliyon (2023). https://doi.org/10.1016/j.heliyon.2023.e15848
7. Kumaran, A.; Vashishth, R.; Singh, S.; Surendran, U.; James, A.; Chellam, P.V.: Biosensors for detection of organophosphate pesticides: current technologies and future directives. Microchem. J. **178**, 107420 (2022)
8. Dhull, V.; Gahlaut, A.; Dilbaghi, N.; Hooda, V.: Acetylcholinesterase biosensors for electrochemical detection of organophosphorus compounds: a review. Biochem. Res. Int. (2013). https://doi.org/10.1155/2013/731501
9. Pundir, C.S.; Malik, A.: Bio-sensing of organophosphorus pesticides: a review. Biosens. Bioelectron. **140**, 111348 (2019)
10. Gong, Z.; Huang, Y.; Hu, X.; Zhang, J.; Chen, Q.; Chen, H.: Recent progress in electrochemical nano-biosensors for detection of pesticides and mycotoxins in foods. Biosensors (2023). https://doi.org/10.3390/bios13010140
11. Bucur, B.; Munteanu, F.D.; Marty, J.L.; Vasilescu, A.: Advances in enzyme-based biosensors for pesticide detection. Biosensors (2018). https://doi.org/10.3390/bios8020027
12. Kurbanoglu, S.; Erkmen, C.; Uslu, B.: Frontiers in electrochemical enzyme based biosensors for food and drug analysis. TrAC Trends Anal. Chem. (2020). https://doi.org/10.1016/j.trac.2020.115809
13. Pérez Fernández, B.; Costa García, A.; de la E. -Muñiz, A.: Electrochemical (bio) sensors for pesticides detection using screen-printed electrodes. Biosensors (Basel) **10**(4), 32 (2020)
14. Ramesh, M.; Janani, R.; Deepa, C.; Rajeshkumar, L.: Nanotechnology-enabled biosensors: a review of fundamentals, design principles, materials, and applications. Biosensors (2023). https://doi.org/10.3390/bios13010040
15. Fredj, Z.; Sawan, M.: Advanced nanomaterials-based electrochemical biosensors for catecholamines detection: challenges and trends. Biosensors (2023). https://doi.org/10.3390/bios13020211
16. Bayda, S.; Adeel, M.; Tuccinardi, T.; Cordani, M.; Rizzolio, F.: The history of nanoscience and nanotechnology: from chemical-physical applications to nanomedicine. Molecules (2020). https://doi.org/10.3390/molecules25010112
17. Lee, J.H.; Park, S.J.; Choi, J.W.: Electrical property of graphene and its application to electrochemical biosensing. Nanomaterials (2019). https://doi.org/10.3390/nano9020297
18. Thangamuthu, M.; Hsieh, K.Y.; Kumar, P.V.; Chen, G.Y.: Graphene- and graphene oxide-based nanocomposite platforms for electrochemical biosensing applications. Int. J. Mol. Sci. (2019). https://doi.org/10.3390/ijms20122975
19. Yağmuroğlu, O.; Diltemiz, S.E.: Development of QCM based biosensor for the selective and sensitive detection of paraoxon. Anal. Biochem. (2020). https://doi.org/10.1016/j.ab.2019.113572
20. Arjmand, M.; Saghafifar, H.; Alijanianzadeh, M.; Soltanolkotabi, M.: A sensitive tapered-fiber optic biosensor for the label-free detection of organophosphate pesticides. Sens. Actuators B Chem. (2017). https://doi.org/10.1016/j.snb.2017.04.121
21. Pitschmann, V.; Matějovský, L.; Lobotka, M.; Dědič, J.; Urban, M.; Dymák, M.: Modified biosensor for cholinesterase inhibitors with Guinea green B as the color indicator. Biosensors (Basel) (2018). https://doi.org/10.3390/bios8030081
22. Arjmand, M.; Aray, A.; Saghafifar, H.; Alijanianzadeh, M.: Quantitative analysis of methyl-parathion pesticide in presence of enzyme substrate using tapered fiber optic biosensor. IEEE Sens. J. (2020). https://doi.org/10.1109/JSEN.2020.2968895
23. Di Tuoro, D., et al.: An acetylcholinesterase biosensor for determination of low concentrations of paraoxon and dichlorvos. N. Biotechnol. (2011). https://doi.org/10.1016/j.nbt.2011.04.011
24. Nesakumar, N.; Sethuraman, S.; Krishnan, U.M.; Rayappan, J.B.B.: "Electrochemical acetylcholinesterase biosensor based on ZnO nanocuboids modified platinum electrode for the detection of carbosulfan in rice. Biosens. Bioelectron. (2016). https://doi.org/10.1016/j.bios.2015.11.010
25. Turan, J., et al.: An effective surface design based on a conjugated polymer and silver nanowires for the detection of paraoxon in tap water and milk. Sens. Actuators B Chem. (2016). https://doi.org/10.1016/j.snb.2016.01.034
26. Kaur, J.; Malegaonkar, J.N.; Bhosale, S.V.; Singh, P.K.: An anionic tetraphenyl ethylene based simple and rapid fluorescent probe for detection of trypsin and paraoxon methyl. J. Mol. Liq. (2021). https://doi.org/10.1016/j.molliq.2021.115980
27. Akdag, A.; Işık, M.; Göktaş, H.: Conducting polymer-based electrochemical biosensor for the detection of acetylthiocholine and pesticide via acetylcholinesterase. Biotechnol. Appl. Biochem. (2021). https://doi.org/10.1002/bab.2030
28. Hidayah et al., N.M.S.: Comparison on graphite, graphene oxide and reduced graphene oxide: synthesis and characterization, In: AIP conference proceedings, AIP Publishing (2017)
29. Perumbilavil, S.; Sankar, P.; Priya Rose, T.; Philip, R.: White light Z-scan measurements of ultrafast optical nonlinearity in reduced graphene oxide nanosheets in the 400–700 nm region. Appl. Phys. Lett. **107**, 051104 (2015)
30. Romero-Arcos, M.; Pérez-Robles, J.F.; Guadalupe Garnica-Romo, M.; Luna-Martinez, M.S.; Gonzalez-Reyna, M.A.: Synthesis and functionalization of carbon nanotubes and nanospheres as a support for the immobilization of an enzyme extract from the mushroom Trametes versicolor. J. Mater. Sci. **54**(17), 11671–11681 (2019)